Line broadening of the $3s_2$-$2p_n$ laser transitions of neon*†

J. W. Knutson, Jr. and W. R. Bennett, Jr.
Dunham Laboratory, Yale University, New Haven, Connecticut 06520
(Received 15 July 1974; revised manuscript received 29 July 1975)

Doppler and collision broadening were studied on six $2p^5 5s \rightarrow 2p^5 3p$ transitions of Ne I. Line-broadening parameters were extracted using the method of least squares in the computer analysis of spontaneous emission profiles transmitted through a scanning plane-parallel Fabry-Perot interferometer. ^{20}Ne-^{4}He and ^{20}Ne-^{20}Ne Lorentz broadening parameters are tabulated, and their temperature dependence summarized.

I. COMPUTER ANALYSIS OF SPONTANEOUS EMISSION PROFILES

We have developed a new method for analyzing line profiles and determining line-profile parameters of atomic transitions. This method involves the computer analysis of spontaneous emission profiles transmitted through a scanning plane-parallel Fabry-Perot interferometer. By analyzing large numbers of points (≈500 over slightly more than one-free spectral range of the Fabry-Perot) in terms of an exact expression for the transmission of a Voigt profile as seen through a Fabry-Perot, one can measure line-profile parameters with an accuracy unobtainable by other methods. In particular, our approach avoids the complications and limitations of laser hole-burning methods.[1–5] Computer analysis of the observed spontaneous emission using the method of least-squares provides "best-fit" line-shape parameters[6] and permits testing alternative line-profile theories.

A. Analysis

The intensity transmitted through a plane-parallel Fabry-Perot interferometer from a monochromatic normal-incidence plane wave is well known to be [7]

$$I(\nu,\nu_i) \propto \{1 - 2R_0 \cos[2\pi(\nu - \nu_i)/(c/2l)] + R_0^2\}^{-1}, \tag{1}$$

where $R_0 = (R_1 R_2)^{1/2}$ is the average mirror reflectance, ν_i a particular interferometer resonance, and $c/2l$ the frequency spacing between interferometer resonances.

For a general spectral response function $f(\nu,\nu_0)$ the intensity transmitted through the Fabry-Perot is of the form

$$dI(\nu_i,\nu_0) \propto \int_\nu f(\nu,\nu_0) I(\nu,\nu_i)\, d\nu\,. \tag{2}$$

Further, if one allows for a distribution $\rho(\nu_m,\nu_0)$ of atoms with different resonant frequencies in respect to ν_m (e.g., the center of the Doppler distribution), the total transmitted intensity through the Fabry-Perot becomes

$$I(\nu_i,\nu_m) \propto \int_{\nu_0} d\nu_0 \rho(\nu_0,\nu_m) dI(\nu_i,\nu_0)\,. \tag{3}$$

For the special case of a Voigt profile, $f(\nu,\nu_0)$ is a Lorentzian spectral-response function, $\rho(\nu_m,\nu_0)$ is a Doppler response function, and Eq. (3) can be integrated in closed form,[8,9]

$$I_T(z) \propto 0.5 + \sum_{n=1}^{\infty} (R_0 e^{-L})^n e^{-n^2 D^2/4} \cos nz\,, \tag{4}$$

where $L = \pi\Delta\nu_L/(c/2l)$, $D = \pi\Delta\nu_D/[(\ln 2)^{1/2}(c/2l)]$, $z = 2\pi(\nu_m - \nu_i)/(c/2l)$, Z is the Fabry-Perot mirror spacing, and $\Delta\nu_L$, $\Delta\nu_D$ are the Lorentz and Doppler *full* widths at half-maximum response.

The rapidity with which the sum in expression (4) converges depends upon R_0, $\Delta\nu_L$, $\Delta\nu_D$, and $c/2l$. For argon ion transitions ($R_0 = 0.85$, $\Delta\nu_L > 750$ MHz, $\Delta\nu_D \approx 4000$ MHz, $c/2l = 15\,000$ MHz),[6] the series converges adequately for experimental analysis in fewer than seven terms. For the $3s_2$-$2p_n$ neutral neon transitions ($R_0 = 0.65$, $\Delta\nu_L > 25$ MHz, $\Delta\nu_D \approx 1500$ MHz, $c/2l = 15\,000$ MHz), the series converges adequately within twelve terms.

B. Experimental method

As the Fabry-Perot interferometer is scanned over slightly more than one free spectral range, we measure the transmitted intensity at ≈500 equally spaced intervals. Analyzing these data points in terms of a five-parameter weighted least-squares fit with expression (4), we are able to determine collision-broadened Lorentz and Doppler widths even when the Lorentz width is a small fraction of the Doppler width (for example, 50 out of 1500 MHz). Previous studies of broadening in spontaneous emission have depended upon

special experimental conditions to increase the ratio of Lorentz width to Doppler width. This increased ratio has been achieved either by cooling the discharge to reduce the Doppler width[10] or by increasing the pressure to broaden the Lorentz width.[11,12] More recent laser hole-burning experiments designed to measure line profiles have been limited to those atomic transitions which will support stable, single-frequency lasers. (Most currently available dye lasers still do not have the required stability to make this type of measurement.)

Our experimental apparatus is shown in Fig. 1. Light from the discharge passes through the scanning Fabry-Perot to the spectrometer and photomultiplier. A computer-controlled digital voltmeter (DVM) measures the intensity-dependent voltage produced by the photomultiplier output current, and each voltage measurement is stored in the computer as a data point (see Fig. 2). The computer completely controls the acquisition and analysis of the data. The computer is operated in an interrupt mode in which it analyzes one data set in between gathering data points for the next set.

The accuracy of the determination of profile parameters is seriously affected by very minute differences between the intensity transmitted by the scanning Fabry-Perot and the intensity measured by the data-gathering apparatus. In order to minimize these differences, numerous procedures are followed.

The most serious source of possible error is the spectrometer. Not only scattered light, but also multiply-diffracted light[13] (a liability of all plane-grating spectrometers) can easily become a part of the data. Our solution to the problem of multiply-diffracted light consists of putting a second grating in the light path to allow only a narrow band (20 Å) of wavelengths to enter the

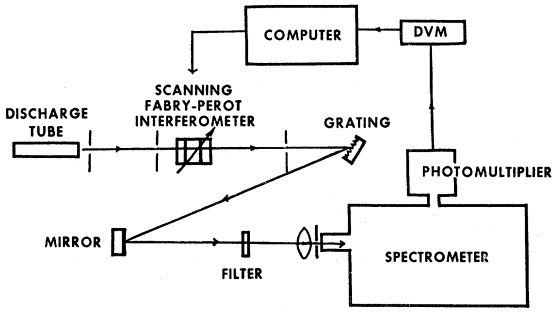

FIG. 1. Schematic diagram of the experimental apparatus for studying line profiles.

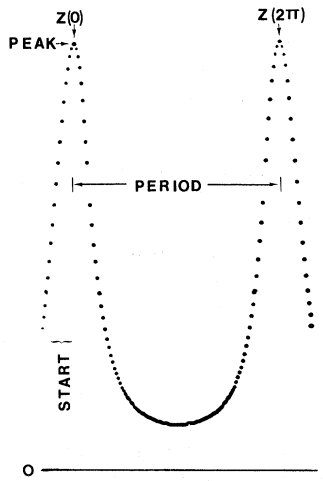

FIG. 2. Schematic representation of data taken in one run. Computer starts taking data after the phototube response has gone through a minimum and takes enough points (typically ≈500) to insure going through two peaks. Computer program then does a five-parameter least-squares fit to the start location, the peak height, the period, the Lorentz width, and the Doppler width.

spectrometer. This technique reduces scattered light by several orders of magnitude and eliminates multiply-diffracted light at the exit slit of the spectrometer.

It is desirable to isolate the spectral line under study without altering its spectral profile. This objective is not always possible in principle with closely spaced lines. In order to study this problem, we did computer simulations of the transmission of a Voigt spectral profile through a spectrometer assuming several different types of spectrometer response functions (see Fig. 3). For example, if one assumes a triangular response whose full width at half-maximum (0.36 Å) is over 20 times the Doppler width and over 100 times the Lorentz width in our Voigt profile for neutral neon, the analyzed value of the Lorentz width is only two-thirds as large as the input value of the Lorentz width. The computed results for the triangular response function were in good agreement with experimental measurements.

To minimize the effect of the spectrometer response, we altered the spectrometer slits to give a trapezoidal response. With a flat response over 1.8 Å (100 times the Doppler width for neutral neon), and a trapezoidal base (3.6 Å) narrow enough to exclude neighboring lines, we were able to transmit accurate Voigt profiles through the spectrometer.

A problem common to all experiments employing a scanning Fabry-Perot interferometer is the

difficulty of maintaining scanning linearity. Our solution to this problem was to let gas leak in from a high-pressure (≥2000 lb/in.^{2}) nitrogen tank through a very fine needle valve into the Fabry-Perot housing at atmospheric pressure. The rate of gas flow is then proportional to the difference in pressure on the two sides of the needle valve. Thus, for a total change in pressure of 1 lb/in.^{2}, this technique provides a nonlinearity of less than 0.1% over the scanning range.

The photodetector is another potential contributor to nonlinearity. We used a high-gain RCA 7265 14-dynode photomultiplier, and employed several techniques to improve the linearity over the normal 3% rating provided by the manufacturer. The photomultiplier was operated in a grounded-anode configuration and the cathode was magnetically and electrically shielded. Our most satisfactory method of measuring nonlinearity consisted of collecting and analyzing line-shape data at the upper and lower bounds of acceptable intensities. All experimental conditions were left the same except that we introduced a broadband filter to reduce intensity at the detector. The scatter in the values of analyzed parameters increased as the intensity decreased, but the line-shape parameters averaged to the same values with the present apparatus and method.

The main effect of misalignment of the Fabry-Perot mirrors is to increase the apparent Doppler width. Results are given in Table I for several different degrees of Fabry-Perot mirror alignment. These results agree with similar measurements by Kuhn and Vaughan[10] for the effect of mirror misalignment on Voigt profile analysis. In our research, the Fabry-Perot mirrors were maintained parallel within $\frac{1}{80}\lambda$ over the central beam aperture. A laser was used to align the Fabry-Perot mirrors parallel to within $\frac{1}{10}\lambda$ at the edge of the mirrors. This method of alignment insured that the mirrors (which were flat to better than $\frac{1}{100}\lambda$ over a 1-in.-diam circle) were parallel to within $\frac{1}{80}\lambda$ over the center 4-mm aperture.

The isotopic purity of the gases producing the spectral line under study is important because very small shifts in wavelength between two isotopes will affect the analysis. The neon-20 used in our experiment was supplied by Mound Laboratories and was certified as 99.9992% neon-20 isotopic composition and 99.9% neon (0.095% hydrogen) gross composition. The helium-4 was Airco reagent-grade helium. Both the neon and the helium were gettered with barium to remove impurities. The discharge tube and gases were connected to a bakeable high-vacuum mercury system with a working vacuum of 10^{-7} Torr and an after-bakeout pressure of about 10^{-8} Torr. Pressures in the experiment were read with a capacitance manometer, calibrated with an oil manometer.

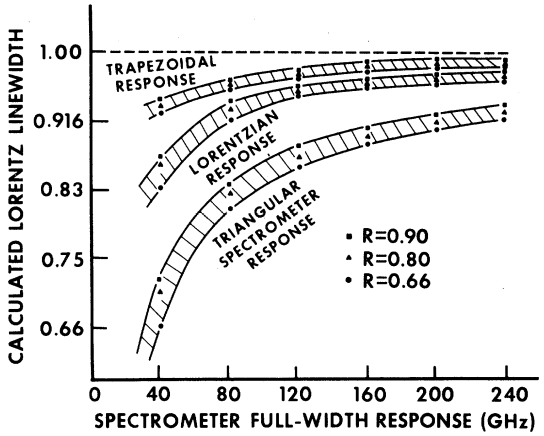

FIG. 3. Effect of spectrometer response function on computed Lorentz width. Best-fit Lorentz widths are shown vs spectrometer slit width (in GHz) for various assumptions for the spectrometer response function. Same initial Voigt profile was assumed in these computer simulations.

One of the profile parameters, the Doppler width, is proportional to the square root of the temperature and caused us to be concerned about the variation in temperature across the discharge tube. The temperature in our discharge tube varied from its hottest at the center of the tube to its coldest at the inside wall of the discharge tube. Doppler measurements taken at the center of the tube and taken halfway between the tube center and the tube wall indicated that the temperature varied by about 4 °C between these two positions. Because this variation was only about one percent of the absolute discharge temperature and because the standard deviations in the temperature measurements were ≈2.5%,

TABLE I. The effect of mirror misalignment on the analysis of Voigt profiles.

Mirror misalignment over the 4-mm central beam aperture	Voigt profile parameters (and their std. dev.) as analyzed by our fitting program. $\Delta\nu_L$ (MHz)	$\Delta\nu_D$ (MHz)
$\frac{1}{80}\lambda$	246 (8)	1683 (14)
$\frac{1}{25}\lambda$	244 (10)	1693 (13)
$\frac{1}{6}\lambda$	224 (16)	2315 (16)

the slight variation in temperature across the discharge tube should not affect our results significantly.

We used a simple heat-transfer calculation and the measured temperature of the outside discharge tube wall to determine the temperature variation ΔT across the tube wall. In particular,

$$\Delta T = X^*U/K = 0.15^* \times 0.25/0.0025 = 15\ ^\circ\mathrm{C},$$

where K is the heat conductivity of quartz tube wall, X the tube wall thickness, and U the input power (cal per unit discharge tube surface area per sec). This calculation, combined with our measurements of the temperature at different points in the discharge and at the outside of the tube, indicates that the temperature differences varied with radius across the discharge tube as shown in Fig. 4. In order to reduce effects of the variation in discharge temperature further, we inserted 4-mm-diam apertures to block all but the central core of the discharge.

A set of experimental data is shown in Fig. 5. These data were taken on the 6118 -Å ($3s_2 \rightarrow 2p_6$) neon transition with a 20:1 mixture of ^{4}He:^{20}Ne and a filling pressure of 2.5 Torr. The analyzed data yielded full Lorentz and Doppler widths of 448(5) MHz and 1467(11) MHz, where the numbers within parentheses are standard deviations for the least-squares fit.

After fitting the parameters, the computer compares the "noise in the fit" (the actual sum of weighted squares) with the expression

$$\sum_i W(i)\{\mathrm{datum}(i) - 0.5[\mathrm{datum}(i+1) + \mathrm{datum}(i-1)]\}^2, \tag{5}$$

which we shall define as the "noise in the data." In the above expression, the summation runs over all data points used in the fit, $W(i)$ is the weighting factor, and datum (i) means the value of the measurement at the ith point. It should be apparent that the ratio of "noise in the fit : noise in the data" will tend to approach a minimum value when you fit the data by the correct theoretical function. Conversely, a very large value of this ratio is a strong indication that the wrong theoretical function has been assumed in the least-squares-fitting procedure. The ratio "noise in fit : noise in data" for the data in Fig. 5 was 0.625, a value representative of those computed in the present experiment.

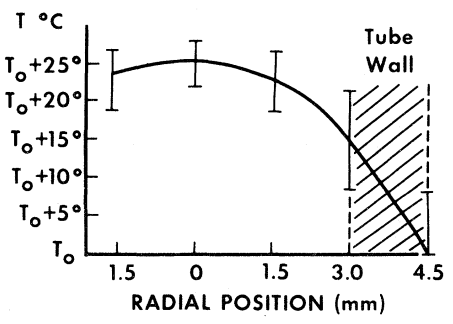

FIG. 4. Temperature variation across the discharge.

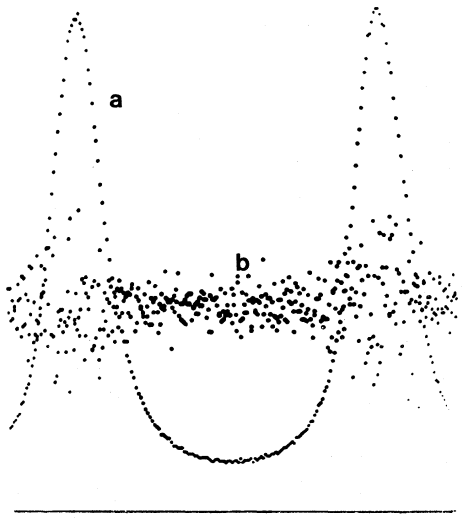

FIG. 5. (a) Data set for the 6118-Å ($3s_2 \rightarrow 2p_0$) neon transition. (b) Gaussian distributed points centered around a line at $\frac{3}{10}$ of the maximum height of the data represent *ten times* the difference between the data and the final theoretical curve.

In order to examine the effect that a speed-dependent asymmetric Voigt profile[14-16] would have upon our measurements, we used the computer to generate such a profile and ran that through our analysis program (see Fig. 6). The average speed of atoms at a given point on the Doppler profile determines the Lorentz width and the frequency shift of light emitted by those atoms (i.e., the broadening and shift depend on the collision probability within the atoms' lifetime). For specific analysis, we assumed the average atomic speed corresponded to a frequency shift of $\Delta\nu_L/2\pi$. For assumed Lorentz and Doppler widths of 400 and 1499 MHz, the analysis program yielded 435 and 1421 MHz. The ratio "noise in fit : noise in data" rose substantially to 8.35, indicating that the theoretical form used to analyze the data in that instance was in-

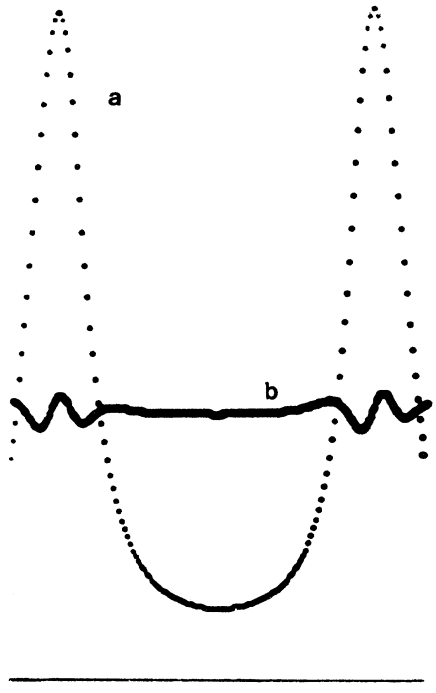

FIG. 6. (a) Computer-generated speed-dependent asymmetric Voigt profile as analyzed by our least-squares program. (b) Ten-times difference between the data and the final theoretical curve. Note the asymmetry in the difference at the peak locations in the Fabry-Perot response.

deed a poor choice.

The speed-dependent profile model which we analyzed was more asymmetrical than one would expect from neon-neon or neon-helium interactions. Even so, the asymmetry, as defined by the frequency difference between the location of the maximum intensity and the center of the profile at half-maximum intensity, is less than 10 MHz. Because none of our present data exhibits as large an asymmetric noise structure in the difference between the data and the best-fit points as that evident in our analysis of the computer-simulated speed-dependent profile (see Fig. 6), we can put an upper limit on the asymmetry of the $3s_2$-$2p_n$ neon transitions of 10 MHz for our experimental conditions (≤ 3 Torr He +Ne).

II. EXPERIMENTALLY MEASURED COLLISION-BROADENING PARAMETERS

Using our method to analyze spontaneous emission profiles, we have determined collision-broadening rates in six of the eight allowed $3s_2$-$2p_n$ neon transitions (Paschen notation). Our results are summarized in Table II. It should be noted that the collision-broadening rates for each transition are the result of computer analysis of over 50 000 individual data points.

The graphs in Figs. 6–8 show experimentally determined Lorentz widths versus gas density for various neon $3s_2$-$2p_n$ transitions. The results increase linearly with the total pressure, and the zero-pressure intercepts for particular transitions all agreed within one standard deviation. We therefore assumed this intercept to be the natural width ($\Delta\nu_N$) for the individual line and have labelled the figures accordingly. However, we were unable to determine quantitatively meaningful values to the natural widths for the $3s_2$-$2p_n$ neon transitions.

The Lorentz width is determined by finding a "best-fit" value for the quantity ($R_0 e^{-L}$) in Eq. (4). Thus a natural width of ≈ 15 MHz for the 6328-Å NeI transition would yield a value of $L_{\text{nat}} \approx 0.003$ when observed with a Fabry-Perot for which $(c/2l) \approx 15$ GHz. In this case, an error in mirror reflectance of $\delta R_0 \approx 0.01$ would result in about a factor of five error in determining the natural width for $R_0 = 0.65$. That is, a fractional error in the determination of the natural width, of amount

$$\frac{\delta(\Delta\nu N)}{\Delta\nu N} \approx \frac{\delta L_{\text{nat}}}{L_{\text{nat}}} \approx \frac{\delta R_0}{L_{\text{nat}} R_0},$$

results from the fractional error $\delta R_0/R_0$ in the mirror reflectance. (Natural widths may, of course, be determined with the present method when either $c/2l$ is small, or $\Delta\nu_N$ is large.)

III. RELATION TO OTHER WORK

Our values for collision-broadening coefficients are given in terms of density and temperature rather than filling pressure as has previously been the common variable. This change is necessary because the Lorentz widths are dependent on the density and, for van der Waals broadening, on the temperature of the discharge as well. Unless the temperature of the discharge and density are both included in collision-broadening measurements, it is impossible to compare results from different experiments.

A number of groups[4,17–21] have measured the broadening of the neon $3s_2$-$2p_4$ transition due to collisions with helium. Unfortunately, most investigators have not specified the gas temperature. One exception occurs with the paper by Mikhnenko *et al.*[21] which reports the broadening of the $3s_2$-$2p_4$ transition in a 5.5 : 1 mixture of He and ^{20}Ne. Translating their results into broadening per 3.25×10^{16} atoms/cm^3 at 295 °K (1 Torr at room temperature), we find that they measured a broadening of 150 MHz (full width)

TABLE II. Collision-broadening parameters for $3s_2 \rightarrow 2p_n$ transitions (Paschen notation) of neutral neon. The numbers represent the increase in full Lorentz width at half-maximum response (in MHz) per Torr at room temperature (3.25×10^{16} atoms/cm^3 at 295 °K).

Wavelength in air (Å)	Lower state	High temperature ^{20}Ne-^{20}Ne ($T\approx370$ °K)	High temperature ^{20}Ne-^{4}He ($T\approx340$ °K)	Low temperature ^{20}Ne-^{4}He ($T\approx165$ °K)
5434	$2p_{10}$	81(13) [a]	130(7)	•••
5939	$2p_3$	•••	133(8)	•••
6046	$2p_7$	106(10)	129(7)	•••
6118	$2p_6$	78(12)	134(7)	105(9)
6328	$2p_4$	94(10)	126(5)	•••
6351	$2p_3$	91(14)	133(7)	•••

[a] Numbers in parentheses within the table represent standard deviations of the least-square-fit values (in MHz). The nominal temperatures at which the data were taken are listed within parentheses at the top of each column.

per Torr. Our results, translated for a 5.5 : 1 He : ^{20}Ne mixture yield a lower value of 121.5 MHz/Torr broadening. Some of the difference between the two values may be explained by their use of the power dip in a single frequency laser to determine collision broadening; this method is extremely sensitive to power broadening and laser cavity adjustment. Another explanation for the difference may be the method they used to measure the discharge temperature. Mikhnenko *et al.* used a thermocouple and a thermometer to measure the temperature of the discharge tube wall, and used heat-transfer theory to calculate the temperature of the gas discharge. In this way,

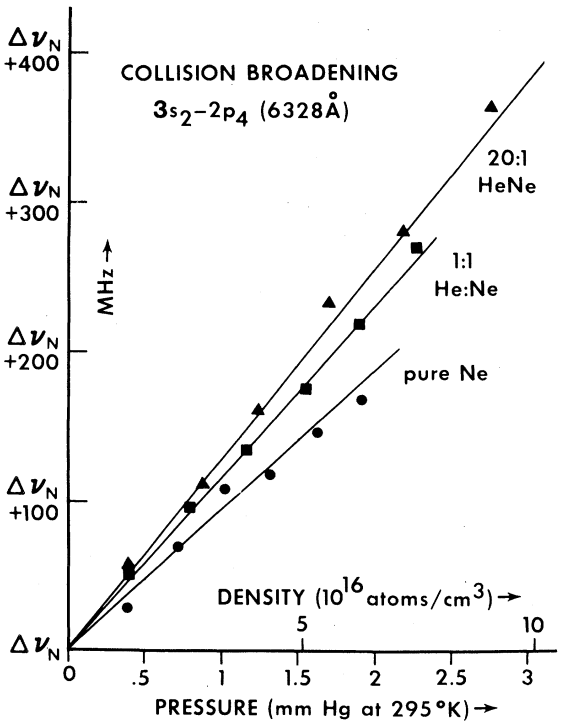

FIG. 7. Experimentally determined Lorentz widths vs density for the neon laser transition at 6328 Å ($3s_2 \rightarrow 2p_4$ transition in Paschen notation). In this figure and in the following ones, only the increase in broadening of the Lorentz width above the natural width ($\Delta\nu_N$) is shown. Values represent the full width at half-maximum response.

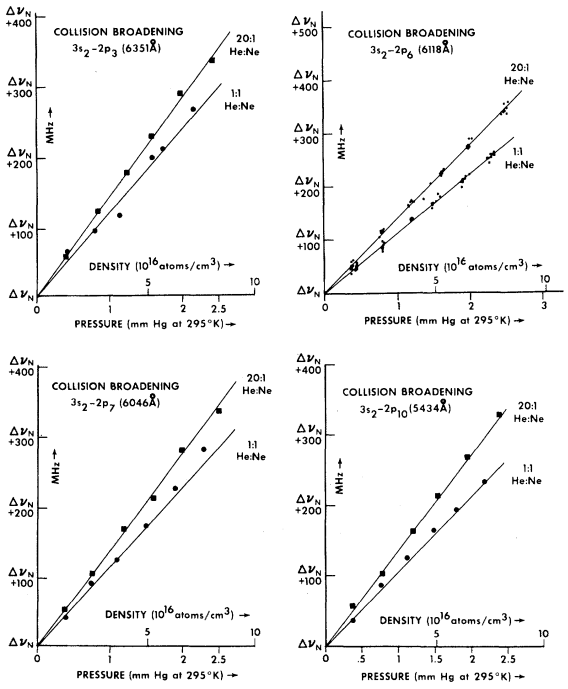

FIG. 8. Pressure-broadening measurements for four other $3s_2 \rightarrow 2p_n$ laser transitions of neon. Transition wavelengths in air are shown in the figure, together with transition assignments in Paschen notation.

they found the gas discharge temperature to be very close (within 30 °C) to that of the bath. Our direct measurements of both the discharge and the tube wall support their measurements for high- and medium-temperature baths, but imply that the discharge temperature may be much higher than the bath at low temperatures.

Smith and Hänsch[20] reported a value of ≈130 MHz/Torr for the broadening on the 6328-Å line in a 7:1 mixture of ^{3}He:^{20}Ne but did not measure the temperature. They estimated the temperature to be 350 °K. A temperature-, mass-, and velocity-dependent conversion of their results made to correspond to our experimental conditions yielded a broadening value of 127 MHz. That number should be compared with our value of 123 MHz/Torr at 295 °K for a 7:1 mixture of ^{4}He:^{20}Ne. Thus these two values appear to agree within the errors of both methods of measurement.

For broadening due to a van der Waals potential (C_0R^{-6}), one expects a broadening temperature dependence of $(T/T_0)^{0.3}$. Hindmarsh *et al.*[22] calculated the effect of using a Lennard-Jones potential ($C_0R^{-6}+C_{12}R^{-12}$) and found that the temperature dependence of the broadening would be of the form $(T/T_0)^x$, where x depends on the transition wave functions. Vaughan and Smith[23] measured the broadening temperature-dependence of the low-lying krypton transition at 7601 Å and found the temperature dependence varied among different perturbers (He, Ne, Ar, and Kr). Measuring the broadening at two different temperatures in a 20:1 ^{4}He:^{20}Ne mixture at 6118 Å (see Fig. 9), we found a ^{20}Ne-^{4}He collision-broadening temperature dependence of $(T/T_0)^{0.33\pm0.03}$. This result is close to the temperature-dependence measured by the Mikhnenko group of $(T/T_0)^{0.34\pm0.04}$.

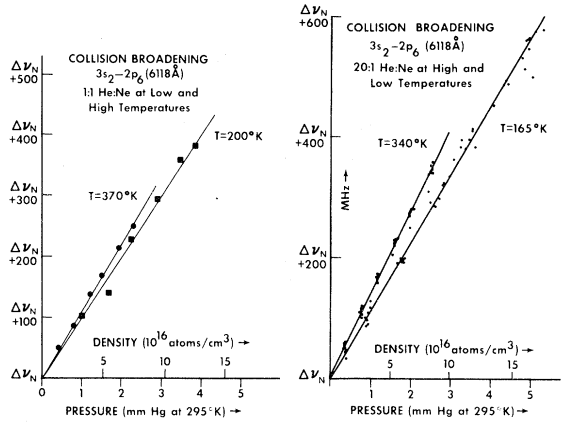

FIG. 9. Variation of collision-broadened Lorentz widths with temperature for the $3s_2 \rightarrow 2p_6$ transition of NeI.

Our measurements of the Ne-Ne interaction at different temperatures show no temperature dependence. This seems to imply that the Ne-Ne interaction is a resonant (C_3R^{-3}) one rather than the van der Waals (C_0R^{-6}) type. This implication is rather surprising because the oscillator strength needed to explain our broadening data would be ≈0.12 instead of ≈0.003 as estimated from the lifetime of the $3s_2$ energy level. However, the $3s_2$-$2p_n$ transitions have very little intensity and tend to be absorbing in pure neon. As a consequence, our broadening measurements may be subject to some uncertain error in the case of pure neon. We hope that future measurements will permit determining the Ne-Ne interaction with greater certainty.

*Research supported in part by the Air Force Office of Scientific Research and the Army Research Office in Durham.

†A preliminary report of the method of analysis used here was given by W. R. Bennett, Jr., J. W. Knutson, Jr., and R. C. Sze, in the *International Symposium on Gas Lasers* (Novosibirsk, USSR, July 1969). A preliminary report of the present experiment was given by J. W. Knutson, Jr., and W. R. Bennett, Jr., Bull. Am. Phys. Soc. 16, 592 (1971), Abstract HC 4.

[1]W. R. Bennett, Jr., V. P. Chebotayev, and J. W. Knutson, Jr., in *Proceedings of the Fifth International Conference on the Physics of Electronic and Atomic Collisions, Leningrad, USSR, 1967* (Nauka, Leningrad, U.S.S.R., 1967), p. 521.

[2]W. R. Bennett, Jr., in *Atomic Physics*, edited by B. Bederson, V. Cohen, and F. Pichanick (Plenum, New York, 1969), pp. 451–454; also see W. R. Bennett, Jr., *Some Aspects of the Physics of Gas Lasers* (Gordon and Breach, New York, 1975).

[3]T. W. Hänsch and P. E. Toschek, IEEE J. Quantum Electron., QE5, 61 (1969).

[4]C. V. Shank and S. E. Schwarz, Appl. Phys. Lett. 13, 113 (1968).

[5]P. W. Smith and R. Hänsch, Phys. Rev. Lett. 26, 740 (1971).

[6]R. Sze and W. R. Bennett, Jr., Phys. Rev. A 5, 837 (1972).

[7]F. A. Jenkins and H. E. White, *Fundamentals of Optics* (McGraw-Hill, New York, 1957), p. 273.

[8]S. Bayer-Helms, Z. Agnew. Phys. 15, 416 (1963).

[9]E. A. Ballik, Appl. Opt. 5, 170 (1966).

[10]H. G. Kuhn and J. M. Vaughan, Proc. R. Soc. A 277, 297 (1964).

[11]H. Margenau and W. W. Watson, Rev. Mod. Phys. 8, 22 (1936).

[12]H. Kuhn, Philos. Mag. 18, 987 (1934).
[13]J. J. Metteldorf and D. O. London, Appl. Opt. 7, 1431 (1968).
[14]W. Voight, K. Bayer Akad, Munchen, Ber., 608 (1912).
[15]F. Reiche, Verh. Dtsch. Phys. Ges. 15, 3 (1913).
[16]P. R. Berman, J. Quant. Spectrosc. Radiat. Transfer 12, 1331 (1972).
[17]P. W. Smith, J. Appl. Phys. 37, 2089 (1966).
[18]W. R. Bennett, Jr., V. P. Chebotayev, and J. W. Knutson, Jr., Phys. Rev. Lett. 18, 688 (1967).
[19]V. N. Lisitsyn and V. P. Chebotayev, Zh. Eksp. Teor. Fiz. 54, 419 (1968) [Sov. Phys.–JETP 27, 227 (1968)].
[20]P. W. Smith and T. Hänsch, Phys. Rev. Lett. 26, 740 (1971).
[21]G. A. Mikhnenko, E. D. Protsenko, E. A. Sedoi, and M. P. Sorokin, Opt. Spectrosc. 29, 65 (1970).
[22]W. R. Hindmarsh, A. D. Petford, and G. Smith, Proc. R. Soc. A 297, 296 (1967).
[23]J. M. Vaughan and G. Smith, Phys. Rev. 166, 17 (1968).